



Hardware Reverse Engineering Workshop (HARRIS 2025)
17.-18. March 2025 Bochum, Germany

Die-Polygon-Capturing: From Hobbyist Hack to Automated Microchip Reverse Engineering Tool

A proof of concept for automating die-polygon-capturing using deep neural networks

Quint van der Linden, Federico Zamberlan, Nevena Rankovic

Tilburg University, Department of Cognitive Science and Artificial Intelligence, The Netherlands



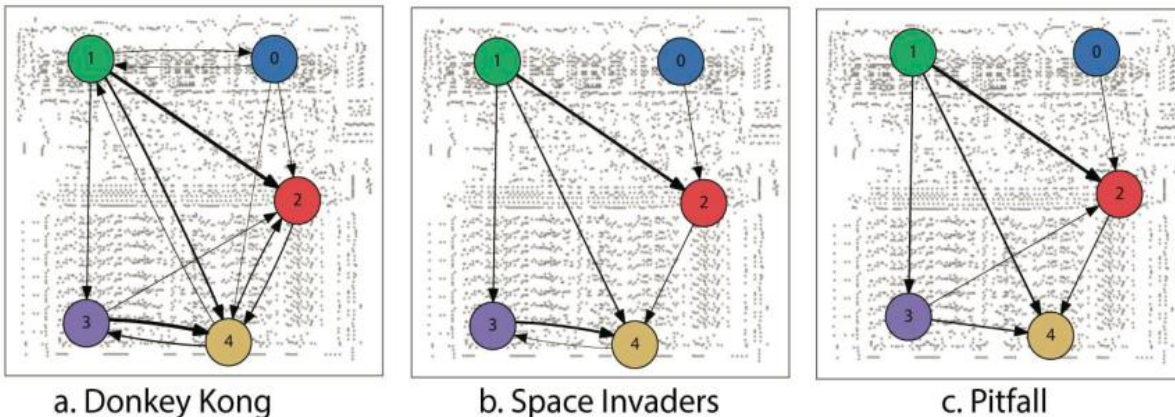
RESEARCH ARTICLE

Could a Neuroscientist Understand a Microprocessor?

Eric Jonas^{1*}, Konrad Paul Kording^{2,3}

1 Department of Electrical Engineering and Computer Science, University of California, Berkeley, Berkeley, California, United States of America, **2** Department of Physical Medicine and Rehabilitation, Northwestern University and Rehabilitation Institute of Chicago, Chicago, Illinois, United States of America, **3** Department of Physiology, Northwestern University, Chicago, Illinois, United States of America

* jonas@eecs.berkeley.edu



Importance of Reverse Engineering Microchips

Some examples

- Enhancing safety and privacy
- Innovative industry influence
- Historical preservation
- Intellectual property infringement detection

A Challenge

A challenge in reverse-engineering microchips

Precisely segmenting the distinct patterns that are printed on the silicon base layer of the chip.

Current Technology and Industry

- Focused Ion Beam (FIB) milling
- Ptychographic X-ray

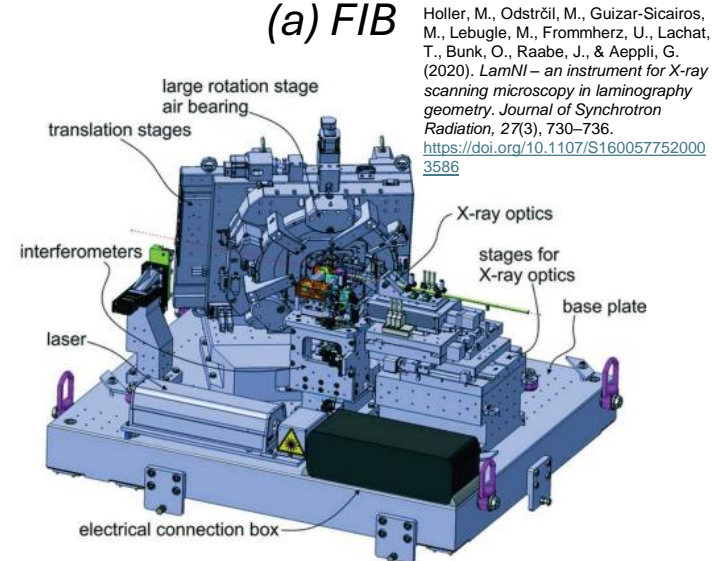
Computed Tomography (PXCT)

- Expensive machinery
- Growing trend of chip designs diversity
- Other approaches to reverse engineering?

Intlvac Thin Film Corporation.
(n.d.). *Nanoquest System – Ion Beam Sputtering and Etching Platform*. Retrieved March 22, 2025, from <https://www.intlvac.com/Systems/intvac-Systems>



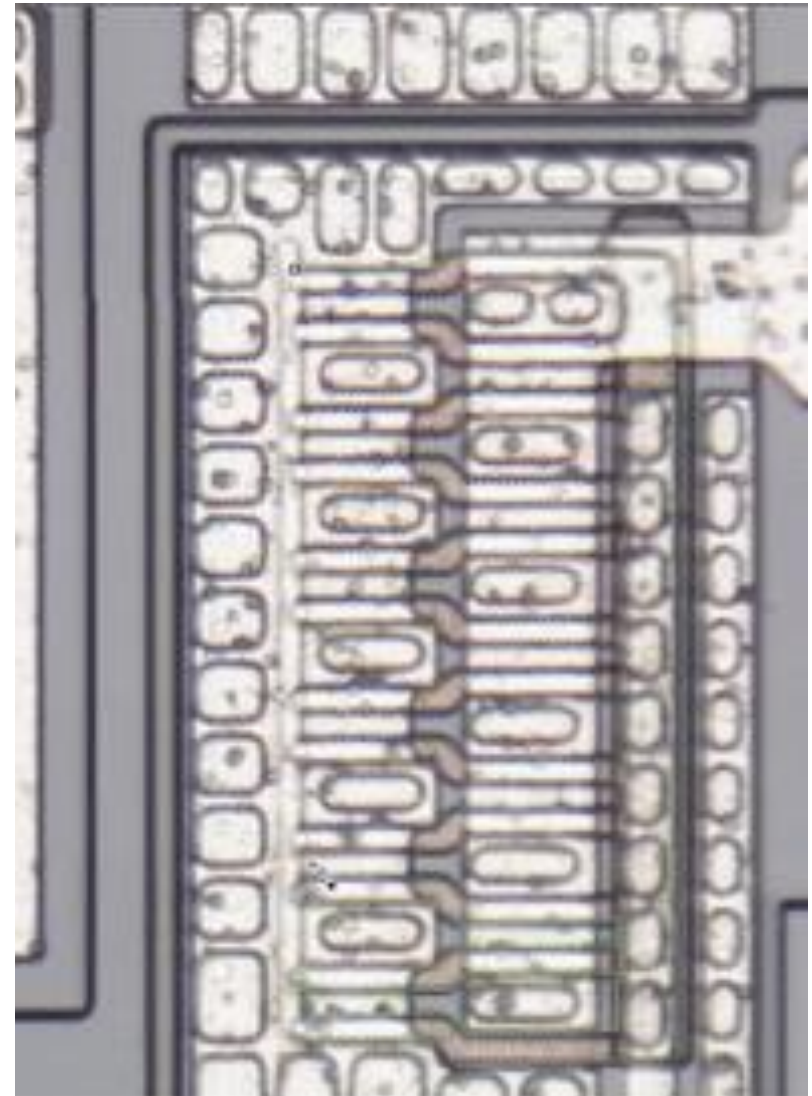
(a) FIB



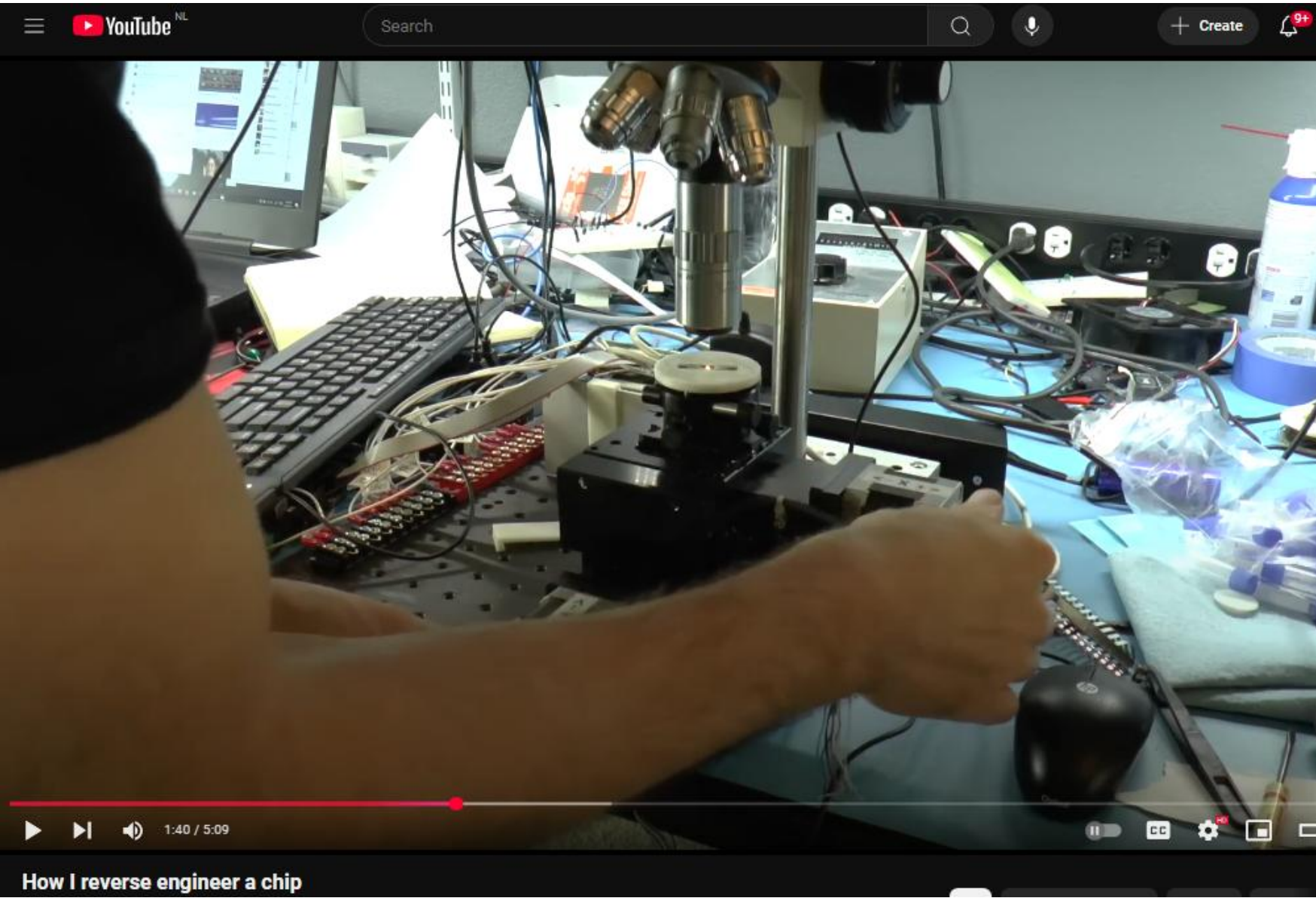
(b) PXCT

Another Approach

- Die-Polygon-Capturing (DPC)
- Effective for simple microchips
- Hobbyist community of engineers
- Cheaper and more accessible
- No scientific literature
- Time-consuming for a person with expert knowledge



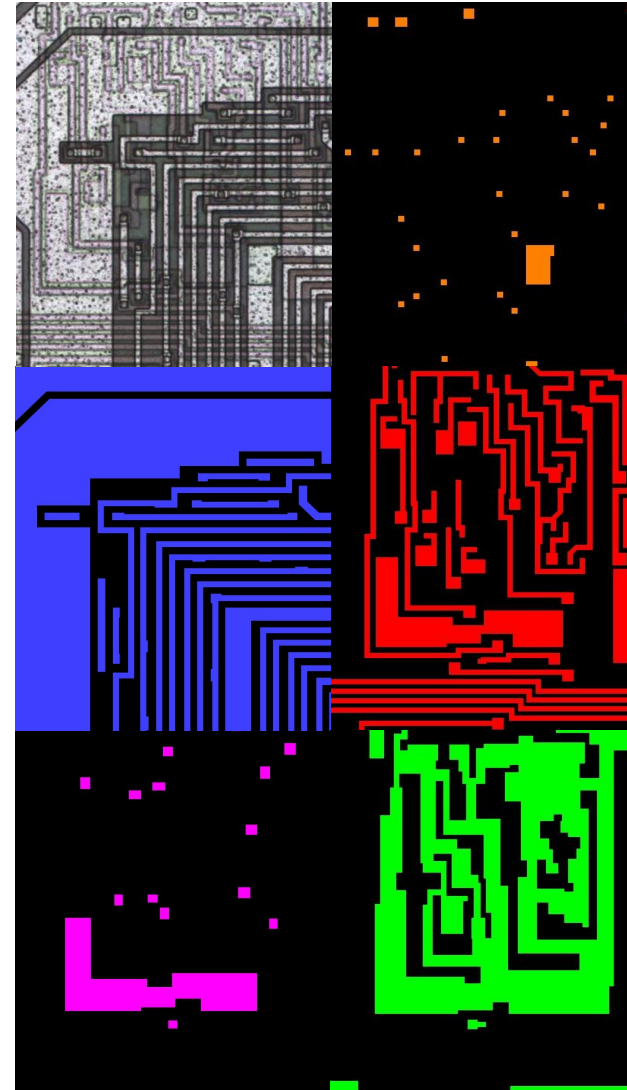
Robert Baruch, "Reverse Engineering a Simple CMOS Chip,"
October 11, 2018, <https://www.youtube.com/watch?v=FMdYuGpPicw>.



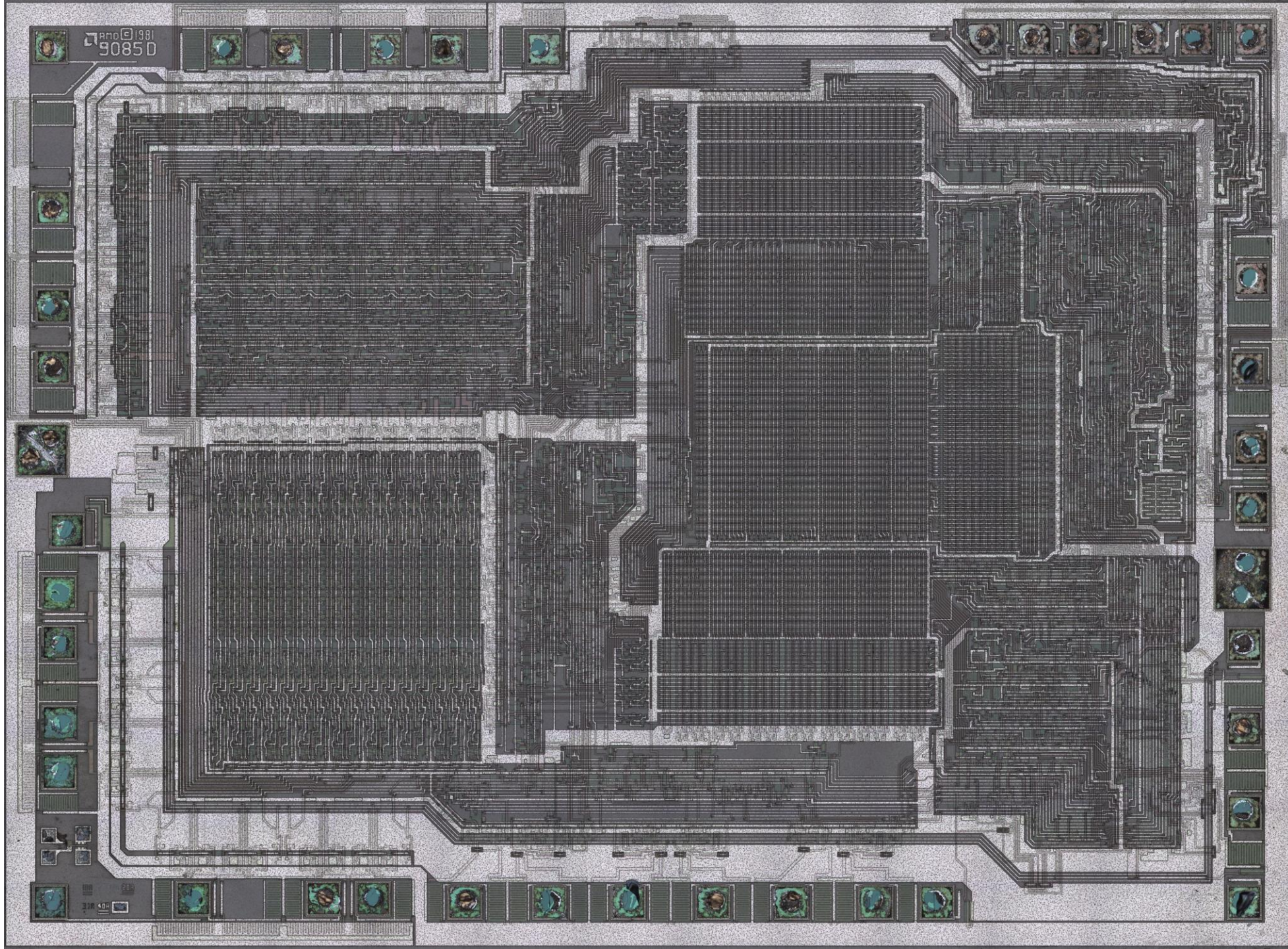
Robert Baruch, "How I Reverse Engineer a Chip," April 23, 2017, <https://www.youtube.com/watch?v=r8Vq5NV4Ens>.

The Dataset

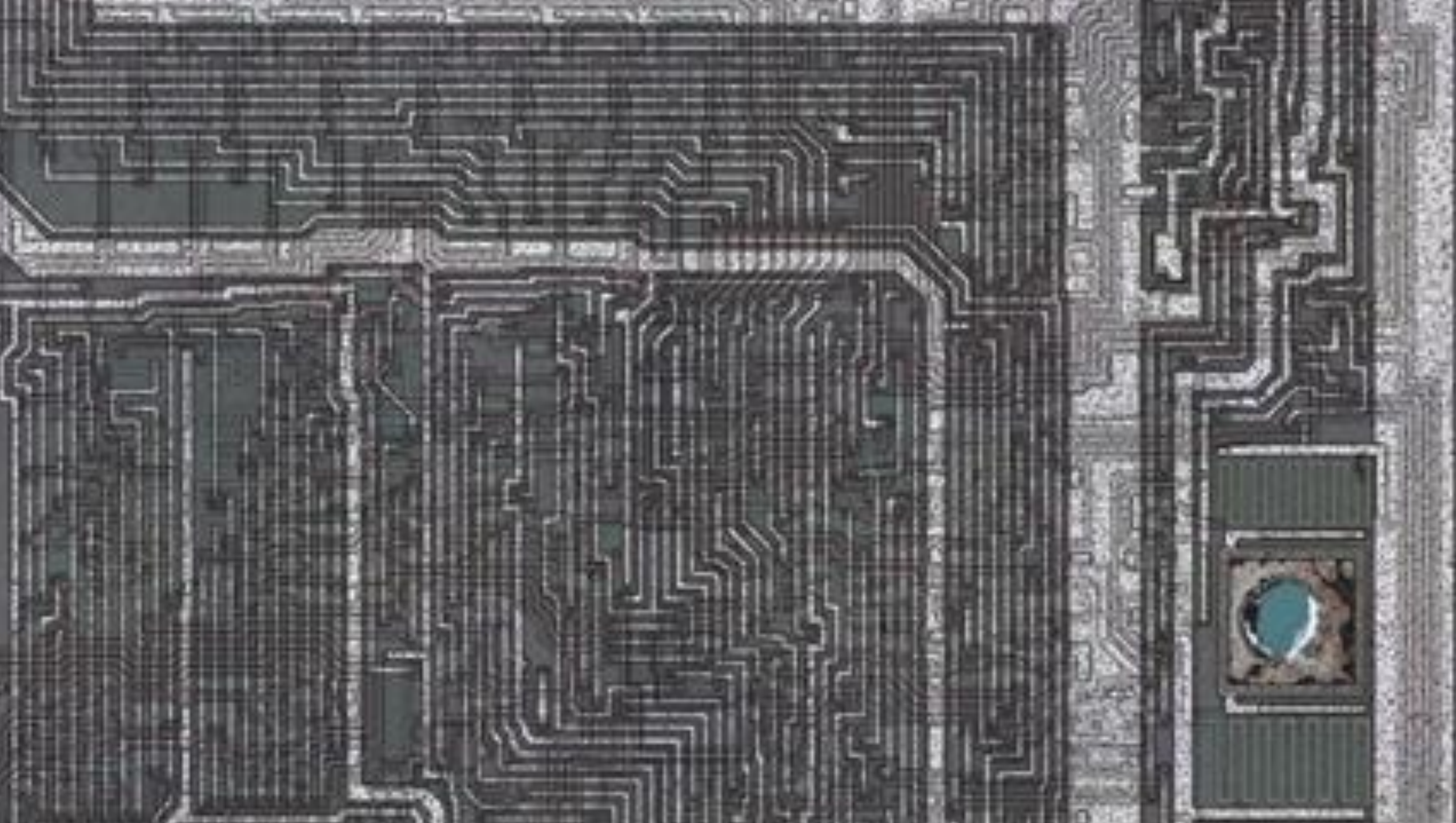
- Blog on Visual6502.org
- AMD 9085D CPU Chip
- Image per label

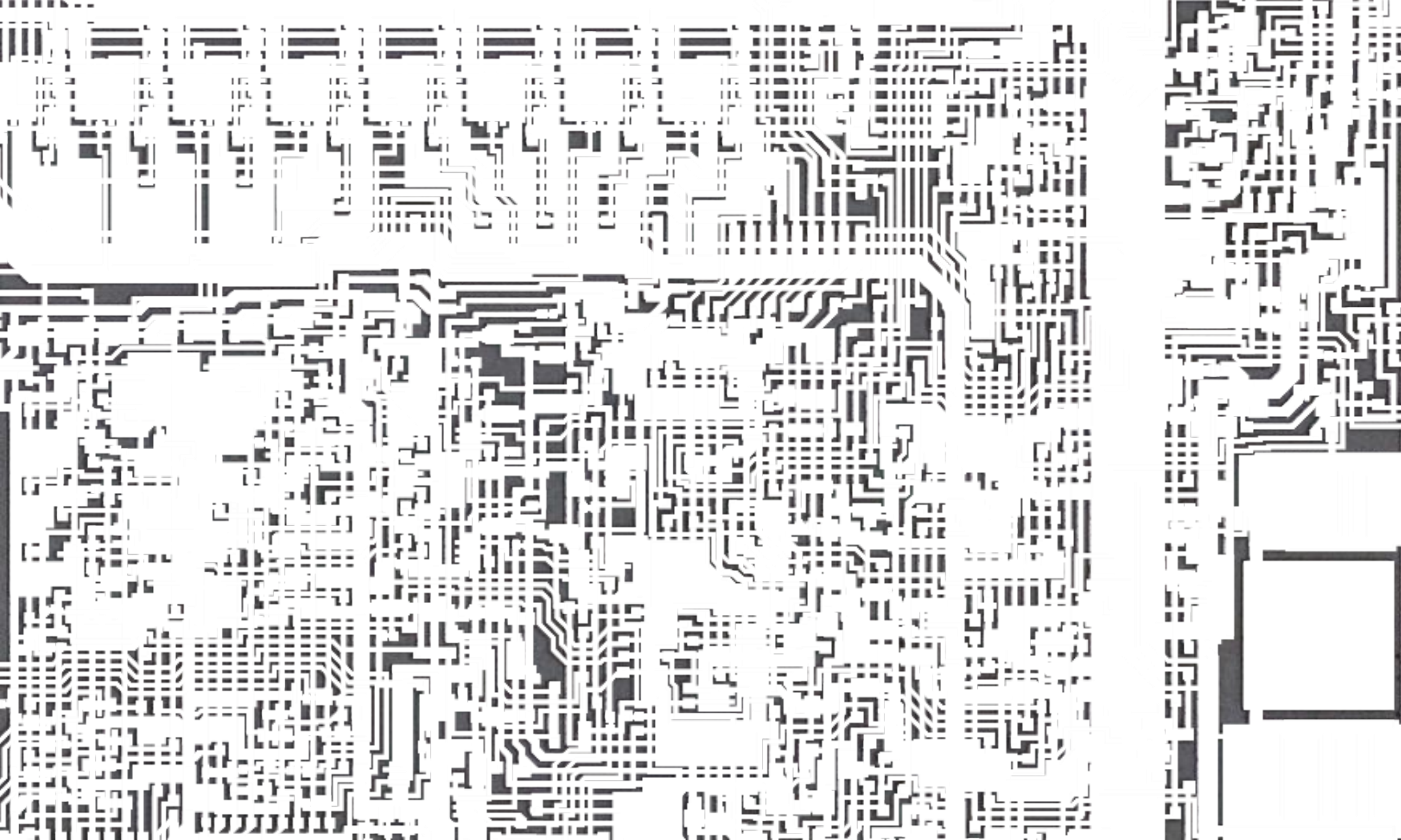


Visual 6502 Project. 8085 Die Shots.
Retrieved from http://visual6502.org/images/pages/8085_die_shots.html



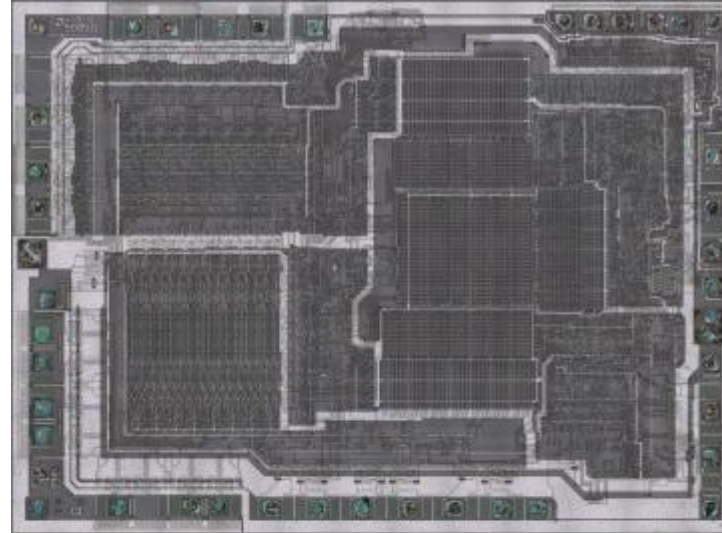
9085D



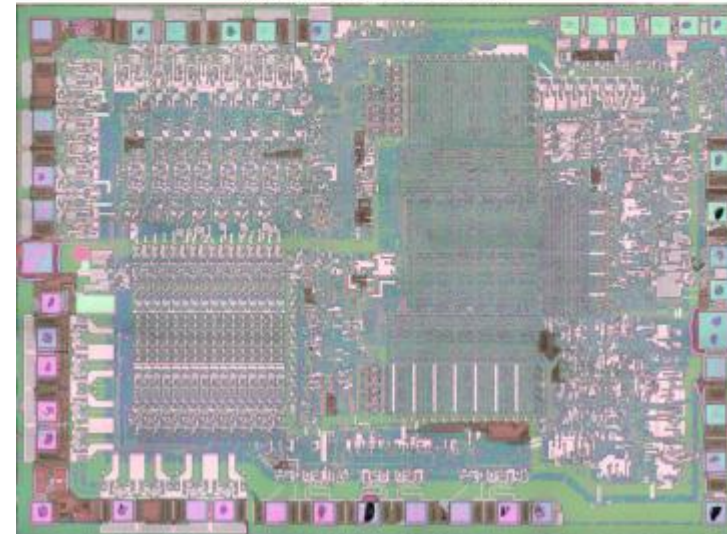


The Dataset

- Blog on Visual6502.org
- AMD 9085D CPU Chip
- Image per label



(a) Surface-level image.



(b) Substrate-level image.

Automating a Time-Consuming Segmentation

- Comparison of neural network model configurations

3

Types of U-Net
architectures

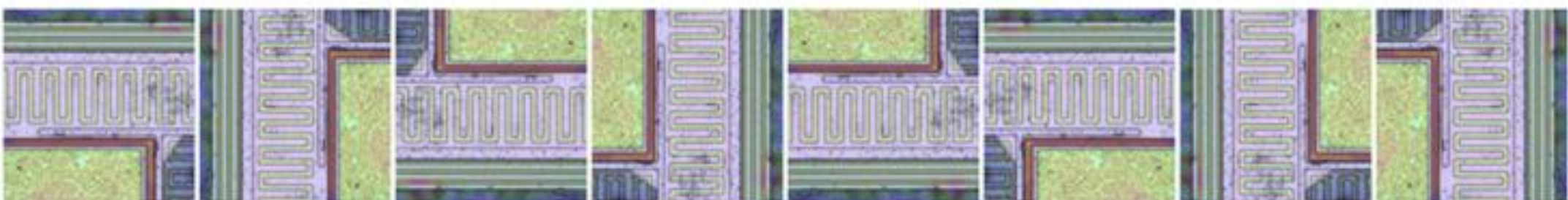
4

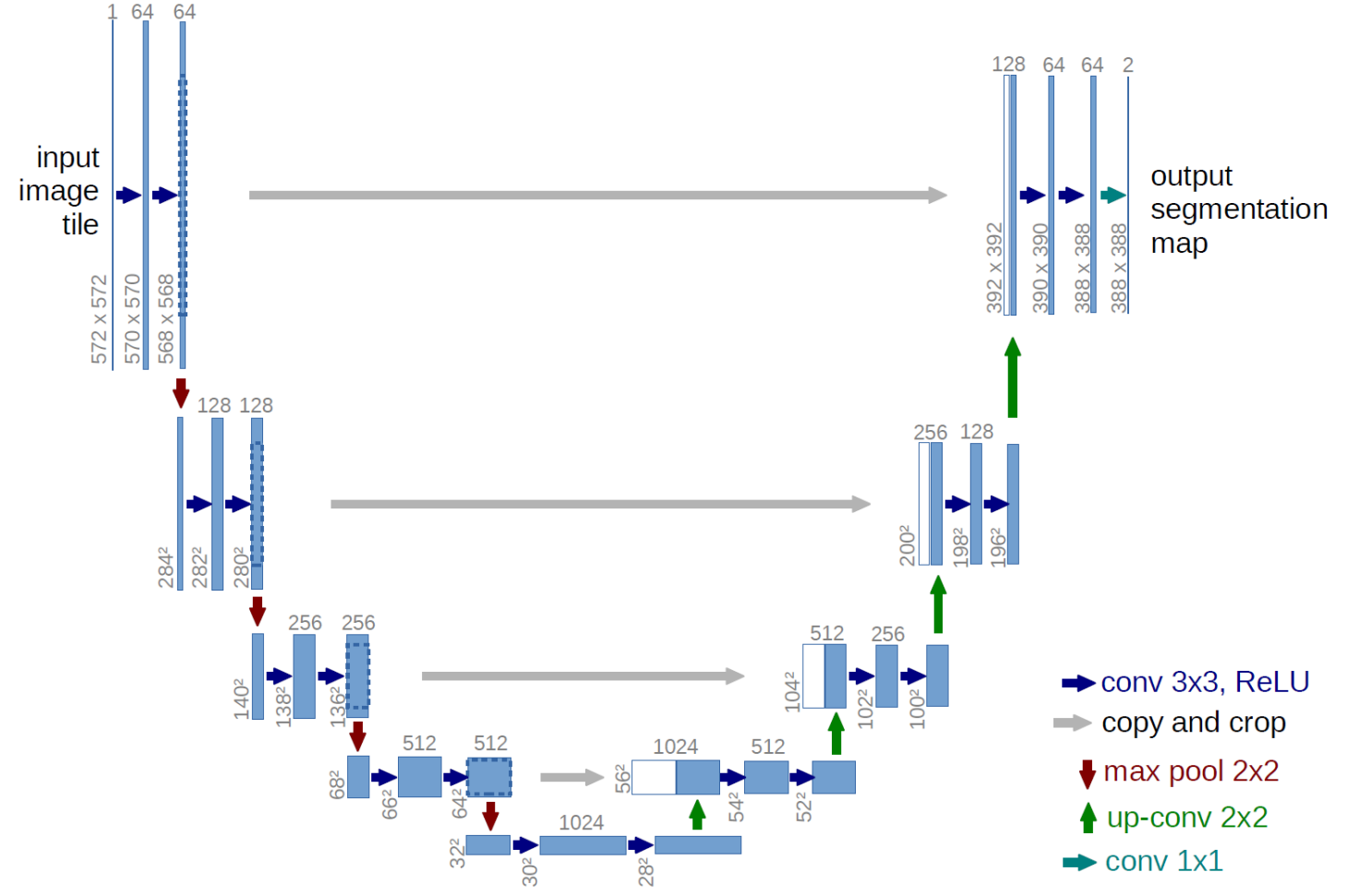
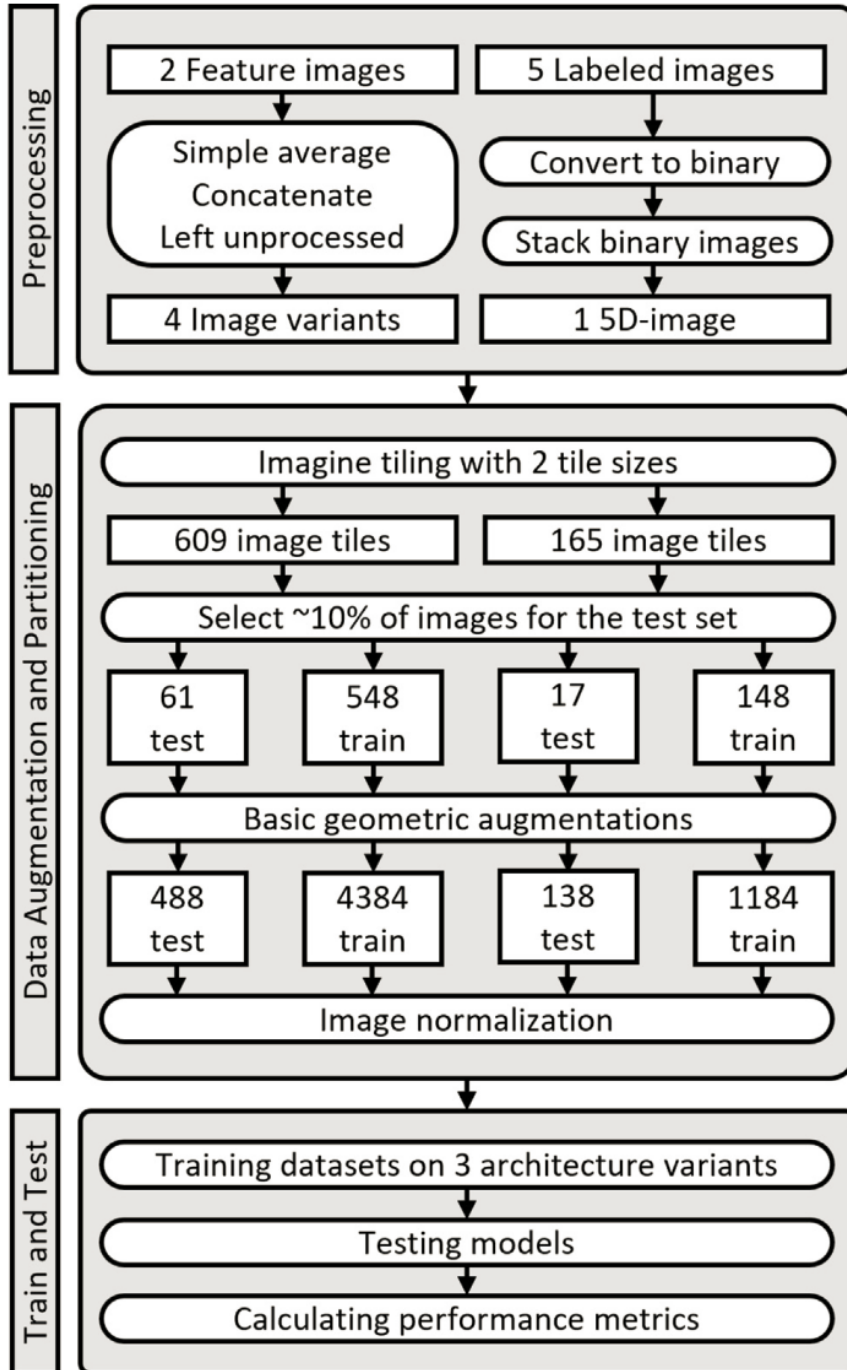
Types of dataset
preprocessing

2

Image sizes

- Extensive data augmentation to enlarge the dataset





Ronneberger, O., Fischer, P., & Brox, T. (2015). *U-Net: Convolutional Networks for Biomedical Image Segmentation*. arXiv preprint arXiv:1505.04597. <https://doi.org/10.48550/arXiv.1505.04597>

PP	Arch	Size	Intersection over Union					F-beta (0.707)					Training Time (h)
			B	D	M	P	V	B	D	M	P	V	
CC	OG	256	71.38	94.47	95.84	87.82	85.55	83.30	97.03	97.78	93.45	92.64	0.83
		512 ^a	44.71	85.58	92.87	81.90	63.30	65.74	94.08	97.06	90.85	78.56	0.36
	P2	256	58.37	94.67	96.06	87.00	85.87	79.18	97.41	98.08	92.71	93.21	0.74
		512 ^a	21.65	87.53	93.84	82.07	41.25	43.46	94.25	96.96	90.24	65.18	0.33
	R	256 ^a	75.52	94.83	96.00	88.11	86.39	86.44	97.48	98.09	93.48	92.22	0.58
		512 ^a	63.19	92.42	95.27	86.03	77.48	78.18	96.29	97.57	92.67	87.31	0.49
	OG	256	77.06	94.54	79.29	87.63	79.09	87.92	97.35	88.88	93.94	89.18	0.81
		512	59.87	91.78	78.45	83.17	72.03	78.45	95.26	87.44	91.76	83.47	0.72
JDE	P2	256	74.15	94.41	72.64	87.43	76.94	84.29	97.02	84.24	93.37	87.56	0.72
		512	41.61	90.61	70.13	82.44	44.19	63.98	94.72	83.65	90.96	68.23	0.65
	R	256 ^a	73.32	94.77	77.60	87.67	79.23	87.16	97.49	87.17	93.87	89.14	0.56
		512 ^a	56.06	91.52	77.01	84.14	72.14	77.81	95.35	86.25	90.72	82.58	0.46
	OG	256	35.75	85.96	96.13	82.13	88.43	58.08	93.61	97.97	90.17	93.59	0.81
		512	3.33	79.82	96.05	79.00	85.57	9.31	90.52	97.81	88.25	91.76	0.72
	P2	256	18.15	77.94	95.20	76.77	78.60	37.30	88.40	97.78	87.86	87.05	0.71
		512	0.00	63.82	95.29	65.89	47.33	0.00	80.24	97.74	83.56	67.77	0.65
	R	256 ^a	38.16	86.41	96.24	79.31	87.68	60.89	92.80	98.21	90.38	93.26	0.55
		512 ^a	4.21	79.21	95.76	77.51	80.04	11.55	88.79	97.83	88.30	89.43	0.46
SA	OG	256	75.36	93.39	95.16	87.02	85.79	86.24	96.40	97.45	92.83	92.60	0.81
		512	57.94	90.97	94.61	84.53	76.54	75.03	95.28	97.18	91.56	87.34	0.72
	P2	256	70.06	93.59	95.33	87.26	83.82	83.74	96.82	97.73	93.43	91.78	0.72
		512	41.74	89.45	93.99	83.09	69.94	64.41	94.75	96.91	90.54	83.63	0.66
	R	256 ^a	70.41	93.52	95.00	87.19	83.18	83.97	96.68	97.32	93.54	91.55	0.55
		512 ^a	51.38	88.88	94.04	82.58	74.03	69.39	94.23	97.19	90.93	85.56	0.46

^a Denotes models utilizing half of the original filter count.

Proof of Concept

- Top performing model configurations show promising results for automation

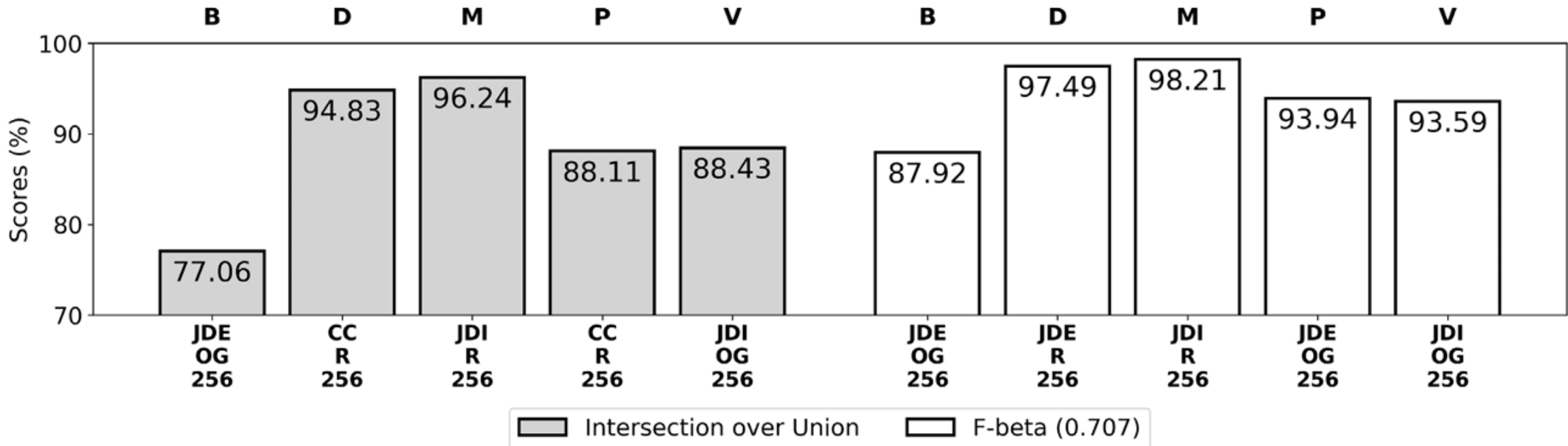
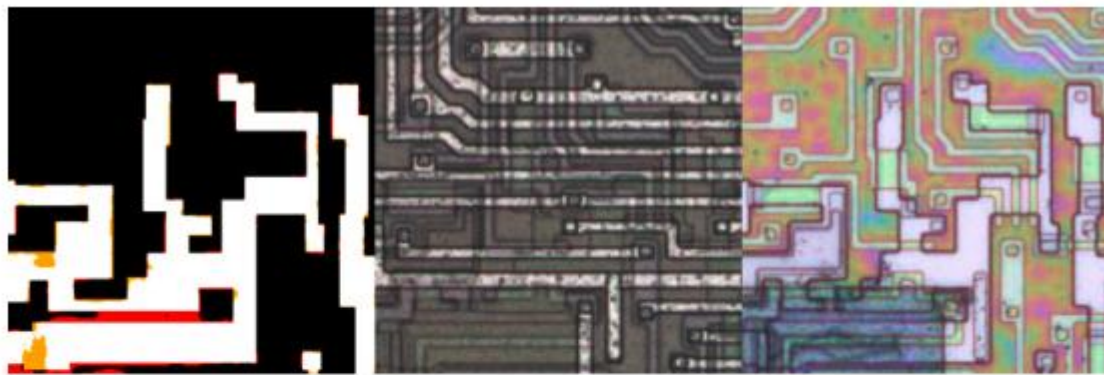


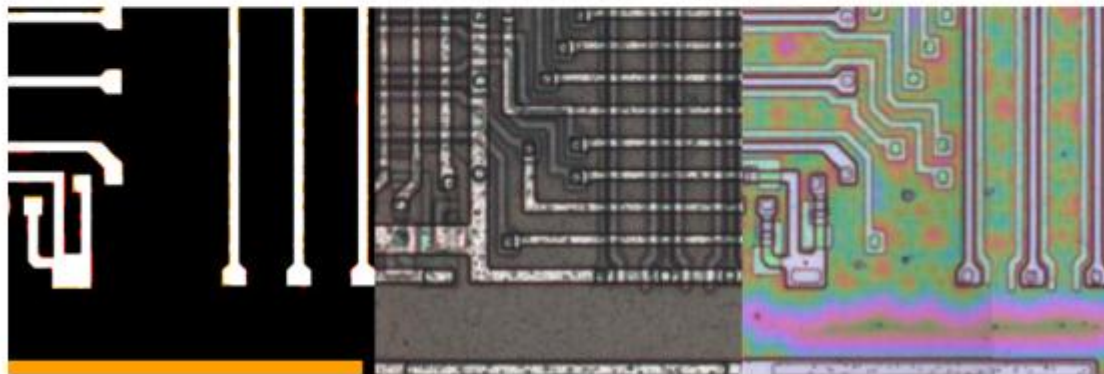
Fig. 10. Bargraph showing the IoU and F-beta (0.707) scores (rounded to 2 d.p.) of the top-performing model settings across labels.

- Error analysis

Largest error-clusters for the **diffusion** label compared to their input (concatenated).



FP-cluster (cs = 705)



FN-cluster (cs = 2717)

Largest error-clusters for the **metal** label compared to their input.



FP-cluster (cs = 874)

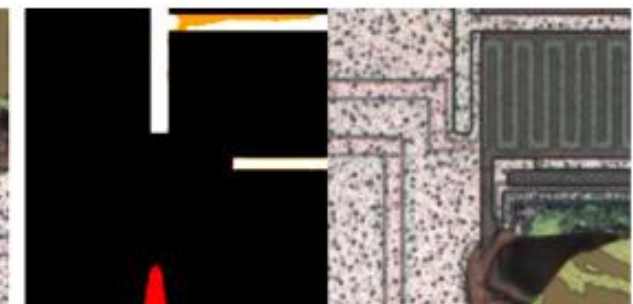


FN-cluster (cs = 508)

Largest error-clusters for the **polysilicon** label compared to their input (concatenated).



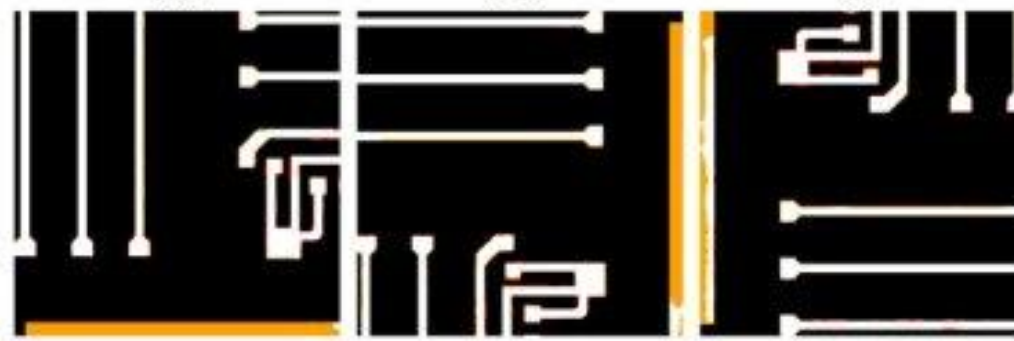
FP-cluster (cs = 643)



FN-cluster (cs = 741)

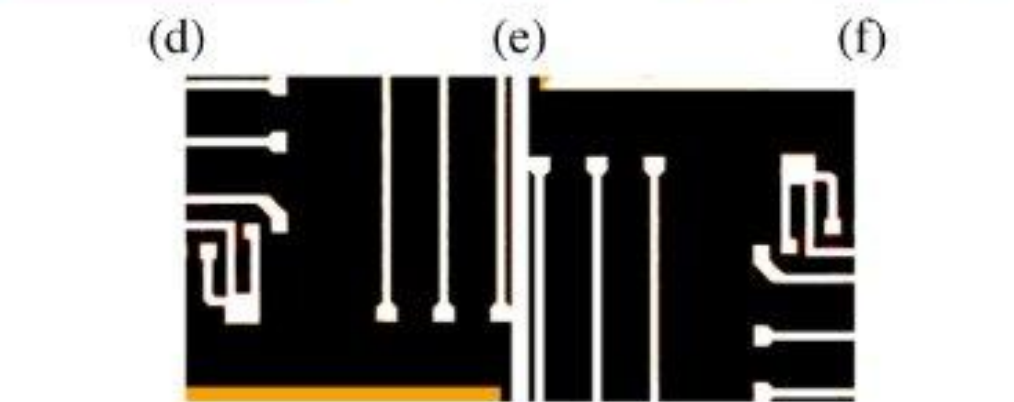


(a)



(b)

(c)



(d)

(e)

(f)



(g)

(h)

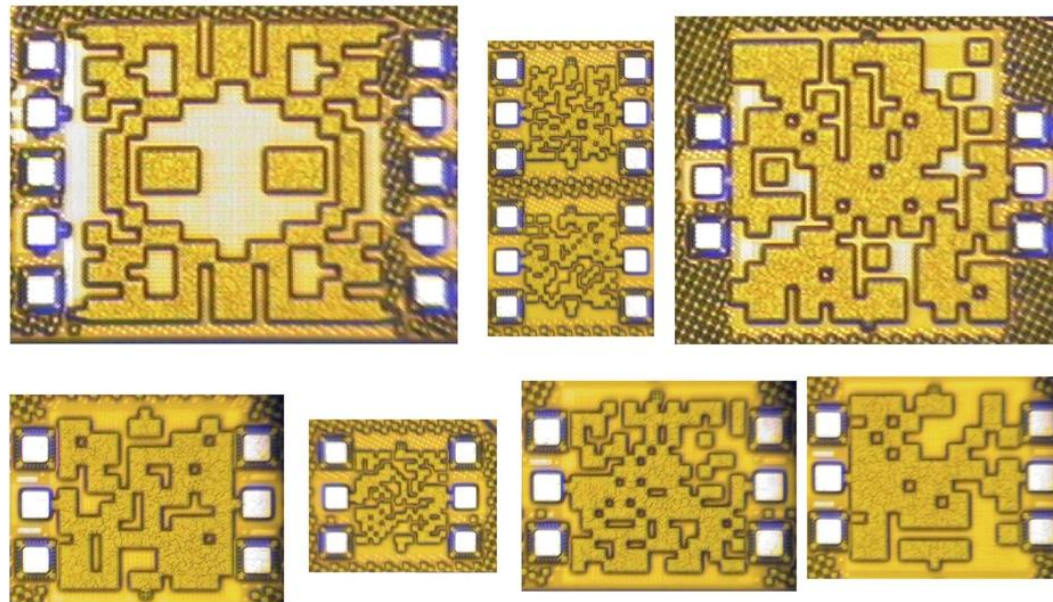
Confusion images of the same augmentation set in the diffusion label.

- Error analysis



Limitations & Future Work

- Generalization
- Encourage to label and open-source microchip designs.
- Unsupervised techniques
- Inspire future research



Article | [Open access](#) | Published: 30 December 2024

Deep-learning enabled generalized inverse design of multi-port radio-frequency and sub-terahertz passives and integrated circuits

[Emir Ali Karahan](#)  [Zheng Liu](#), [Aggraj Gupta](#), [Zijian Shao](#), [Jonathan Zhou](#), [Uday Khankhoje](#) & [Kaushik Sengupta](#)

Nature Communications **15**, Article number: 10734 (2024) | [Cite this article](#)

Karahan, E.A., Liu, Z., Gupta, A. et al. Deep-learning enabled generalized inverse design of multi-port radio-frequency and sub-terahertz passives and integrated circuits. *Nat Commun* **15**, 10734 (2024). <https://doi.org/10.1038/s41467-024-54178-1>

Contact



Quint van der Linden
quint.linden@gmail.com



Nevena Ranković
n.rankovic@tilburguniversity.edu



Federico Zamberlan
f.zamberlan@tilburguniversity.edu

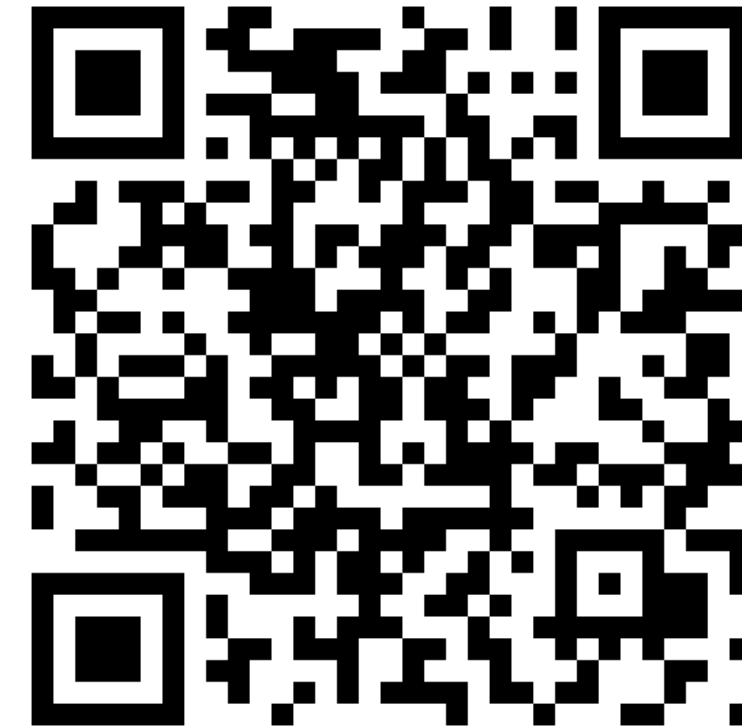


Expert Systems with Applications

Volume 261, 1 February 2025, 125479



Simple integrated circuit reverse-engineering with deep learning:
A proof of concept for automating die-polygon-capturing



DOI: 10.1016/j.eswa.2024.125479

<https://doi.org/10.1016/j.eswa.2024.125479>